Graphene-Assisted Microfiber for Optical-Power-Based Temperature Sensor

Qizhen Sun, Xiaohui Sun, Weihua Jia, Zhilin Xu, Haipeng Luo, Deming Liu, and Lin Zhang

***Abstract*— Combined the large evanescent field of microfiber with the high thermal conductivity of graphene, a sensitive all-fiber temperature sensor based on graphene-assisted microfiber is proposed and experimentally demonstrated. Microfiber can be easily attached with graphene due to the electrostatic force, resulting in an effective interaction between graphene and the evanescent field of microfiber. The change of the ambient temperature has a great influence on the conductivity of graphene, leading to the variation of the effective refractive index of microfiber. Consequently, the optical power transmission will be changed. The temperature sensitivity of 0.1018 dB/°C in the heating process and 0.1052 dB/°C in the cooling process as well as a high resolution of 0.0098 °C is obtained in the experiment. The scheme may have great potential in sensing fields owing to the advantages of high sensitivity, compact size, and low cost.**

***Index Terms*— Microfiber, graphene, evanescent field, temperature sensor.**

I. Introduction

THE PAST decades have seen increasing applications of microfiber in all-fiber filters, sensors and modulators, etc. due to its simple fabrication technique, compact size, low loss, large evanescent field and easy integration with fiber systems [1]. Featured with the advantages of flexibility, small footprint and immunity to electromagnetic interference, all fiber temperature sensors have been widely used in material processing, food testing, greenhouse monitoring and other fields. Zeng et al. achieved a temperature sensitivity of 0.27nm/°C in heating process and −0.28nm/°C in cooling process by utilizing microfiber knot resonator [2]. Luo et al. demonstrated a temperature sensor with the sensitivity as high as −0.98921nm/°C by immersing highly bi-refringent D-shaped microfiber in sucrose solution [3]. However, both of them are difficult to fabricate, as well as require expensive wavelength detecting systems. Considering the limit of resolution of the optical spectrum analyzer, the temperature resolution can just reach to 0.02°C. Zhu et al. proposed a single-mode tapered fiber coated by thermo-sensitive material and the output power monotonically increased 1.2dB with the temperature variation from −20 °C to 80 °C [4]. Harun demonstrated a microfiber-loop-resonator-based temperature sensor with the sensitivity of 0.043dB/°C by detecting the extinction ratio of the comb spectrum [5]. Nevertheless, the achieved results are relatively nonlinear and the sensitivity is not high enough.

On the other hand, graphene has been hailed as a super-thin optical material in electronics and photonics due to its unique valence bands structure and strong inter-band transitions. Based on the mature platform of fiber optics, graphene is especially flexible to be incorporated with fiber as a new composite waveguide, applied as polarization controller [6], wideband saturable absorber [7], and etc. Li et al. reported a graphene-clad microfiber based all-optical modulator at ∼1.5μm with a response time of ∼2.2ps, which could achieve a modulation depth of 38% owing to the enhanced light-graphene interaction [8]. Since the optical conductivity of graphene can be easily influenced by the environment due to its two-dimensional structure, it also has great potential in sensing fields. Xiao et al. demonstrated a reduced graphene oxide based side-polished fiber for humidity sensing with sensitivity of 0.31dB/%RH in high relative humidity range (70-95%) [9]. Yavari et al. employed a macro graphene foam-like network for parts-per-million level detection of NH_3 and NO_2 with good sensitivity and durability [10]. Zhang et al. demonstrated a temperature sensor based on a side-polished fiber coated with reduced graphene oxide film, achieving a high sensitivity of 0.134dB/°C [11]. However, there are few reports on microfiber combined with graphene for temperature sensors yet, which is further miniaturized to be suitable for integration and probe.

In this letter, by taking advantage of the super-high thermal conductivity of graphene, we propose an all-fiber temperature sensor based on graphene assisted microfiber (GAMF). The refractive index of graphene can be changed along with the surrounding temperature, leading to the variation of transmission power of the GAMF. Theoretically analysis and experimental demonstration of the sensor are carried out and achieve high sensitivity higher than 0.1018dB/°C. Meanwhile, GAMF presents special superiorities including easy fabrication, miniaturization and low cost.

Manuscript received September 19, 2015; revised October 15, 2015; accepted October 21, 2015. This work was supported in part by the National Natural Science Foundation of China under Grant 61275004, in part by the Natural Science Foundation of Hubei Province for Distinguished Young Scholars under Grant 2014CFA036, and in part by the European Commission's Marie Curie International Incoming Fellowship under Grant 328263.

Q. Sun is with the National Engineering Laboratory for Next Generation Internet Access System, School of Optical and Electronic Information, Huazhong University of Science and Technology, Wuhan 430074, China, and also with the Aston Institute of Photonic Technologies, Aston University, Birmingham B4 7ET, U.K. (e-mail: qzsun@mail.hust.edu.cn).

X. Sun, W. Jia, Z. Xu, H. Luo, and D. Liu are with the National Engineering Laboratory for Next Generation Internet Access System, School of Optical and Electronic Information, Huazhong University of Science and Technology, Wuhan 430074, China (e-mail: hxsun@hust.edu.cn; whjia@hust.edu.cn; zlxu@hust.edu.cn; luohaipeng@163.com; dmliu@hust.edu.cn).

L. Zhang is with the Aston Institute of Photonic Technologies, Aston University, Birmingham B4 7ET, U.K. (e-mail: l.zhang@aston.ac.uk).

Color versions of one or more of the figures in this letter are available online at http://ieeexplore.ieee.org.

Digital Object Identifier 10.1109/LPT.2015.2495107

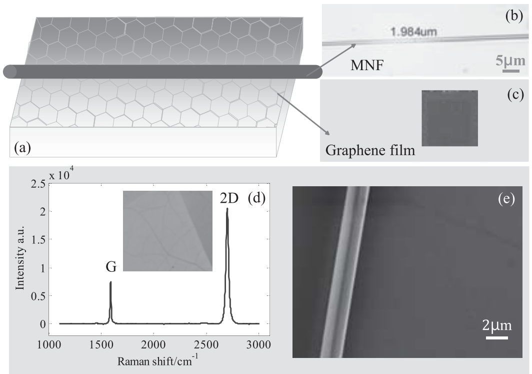

Fig. 1. (a) Schematic of the GAMF; (b) microscope image of bare microfiber; (c) photograph of the graphene film; (d) Raman spectrum of graphene film, inset: the morphology of graphene film; (e) SEM of the GAMF.

II. System Configuration and Working Principle

The structure of the GAMF is schematically depicted in Fig. 1(a), which is a micro/nano fiber strongly attached with a small piece of single-layer graphene film. The microfiber is bilaterally stretched from a standard single-mode-fiber (SMF) by using the flame-heating and taper-drawing technology. The flow rate of hydrogen and the tensile speed are optimized to 106ml/min and 0.6mm/s, respectively, and then the waist diameter of the microfiber is decreased to 1.984μm, as shown in Fig. 1(b) which is obtained from a microscope imaging system. The graphene film is provided by Nanjing JCNANO Technology Co., LTD, which is firstly grown on copper foil through chemical vapor deposition (CVD), and then transferred to the 1cm^2 silica substrate, as illustrated in Fig. 1(c). The single ratio of the graphene film without doping is higher than 90%, which appears as two-dimensional hexagonal lattice with large specific surface area. In the infrared-to-visible spectral range, the constant absorption coefficient and the sheet resistance of the graphene film are 2.3% and 500-800Ω, respectively. From the Raman spectrum of the graphene film presented in Fig. 1(d), the intensity ratio of 2D peak to G peak is far higher than 2, and most part in the morphology is light-colored, demonstrating that the graphene film is single-layer [12].

In order to decrease the transmission loss of microfiber, the graphene film is transferred from the silica substrate to the MgF_2 substrate with lower refractive index. Hold and stretch the microfiber by two three-dimensional alignment stages, and then adjust the stages until the microfiber tightly attached onto the graphene film, to form the GAMF sensor. The scanning electron microscopy (SEM) image of the GAMF with the focus on the microfiber is shown in Fig. 1(e). The clear images of both microfiber and graphene film indicate that the microfiber is closely attracted onto the graphene film, owing to the high evanescent field and electrostatic force between them.

The sensing mechanism is analyzed in theory as follows. When temperature rises, the electron-hole concentration of the graphene will increase due to the thermal excitation, resulting in the rising of the corresponding dynamic conductivity [13]. According to Refs. [14]–[16], the optical conductivity of graphene can be modeled by Kubo formula:

$$\sigma_s(\omega, \mu_c, \tau, T) = -\frac{ie^2(\omega + i\tau^{-1})}{\pi\hbar^2}[\int_{-\infty}^{+\infty} \frac{|\varepsilon|}{(\omega + i\tau^{-1})^2} \cdot \frac{\partial f_d(\varepsilon)}{\partial \varepsilon} d\varepsilon - \int_{0}^{+\infty} \frac{\partial f_d(-\varepsilon) - \partial f_d(\varepsilon)}{(\omega + i\tau^{-1})^2 - 4(\varepsilon/\hbar)^2} d\varepsilon] \quad (1)$$

Where $\hbar$ is the reduced Plank constant, μ_c is the chemical potential, ω is the radiation frequency, ε is the permittivity and T is the temperature. $f_d = \{1 + \exp[(\varepsilon - \mu_c)/(K_B T)]\}^{-1}$ is the Fermi-Dirac distribution, where K_B is the Boltzmann constant. $\tau = \mu_c m_u/(ev_F^2)$ is the momentum relaxation time, where e is the electron charge, $\nu_F \approx 10^8 cm/s$ is the Fermi velocity, $m_u \approx 10^4 cm^2/V \cdot s$ is the impurity-limited DC mobility. The first and second terms in Eq. (1), corresponding to the intra-band electron-photon scattering and the direct inter-band electron transition, respectively, can be evaluated as

$$\sigma_{intra} = i\frac{e^2 K_B T}{\pi\hbar^2(\omega + i\tau^{-1})}[\frac{\mu_c}{K_B T} + 2\ln(\exp(-\frac{\mu_c}{K_B T}) + 1)] \quad (2)$$

$$\sigma_{inter} = i\frac{e^2}{4\pi\hbar}\ln[\frac{2|\mu_c| - \hbar(\omega + i\tau^{-1})}{2|\mu_c| + \hbar(\omega + i\tau^{-1})}] \quad (3)$$

Consequently, the complex conductivity of graphene is

$$\sigma_s(\omega, \mu_c, \tau, T) = \sigma_{intra} + \sigma_{inter} = \sigma_r + i\sigma_i \quad (4)$$

Where σ_r and σ_i are the real part and imaginary part of the conductivity. With the complex effective electrical permittivity $\varepsilon_{eff} = 1 + i\sigma_s/\omega\varepsilon_0 d$ and the refractive index $n = \sqrt{\varepsilon_{eff}}$ [17], [18], the real part of refractive index of graphene can be calculated as

$$n_{gr} = \sqrt{\frac{\sqrt{(\sigma_i - \omega\varepsilon_0 d)^2 + \sigma_r^2} - (\sigma_i - \omega\varepsilon_0 d)}{2\omega\varepsilon_0 d}} \quad (5)$$

Where $\varepsilon_0 = 8.85 \times 10^{-12} F/m$ is the vacuum dielectric constant, and d is the thickness of the graphene. Here, we assume $\omega = 2\pi c/\lambda$, $\lambda = 1550nm$, $c = 3 \times 10^8 m/s$, $d = 1nm$, $T = 0 \sim 100°C$ and then calculate the variations of the conductivity and refractive index of graphene along with the temperature change. From the simulation results in Fig. 2(a) and (b), it is obvious that both the real part and imaginary part of the conductivity are increased with the rise of temperature. Therefore, the real part of the refractive index of graphene is inversely proportional to the temperature with the coefficient of $-7.385 \times 10^{-6}°C^{-1}$ and linearity of 96.94% as depicted in Fig. 2(c).

When the surrounding temperature changes, both of the MgF_2 substrate and graphene film will affect the effective refractive index of the MNF. However, the thermo-optic coefficient of MgF_2 is around $3.2 \times 10^{-7}°C^{-1}$ when the operating wavelength is set from 1.15μm to 3.39μm [19], which is much smaller than that of the graphene. Therefore, the effect of the temperature on MgF_2 can be negligible.

In order to analyze the effect of n_{gr} on the optical field distribution of the GAMF, we use the finite element method—COMSOL to numerically calculate the effective refractive

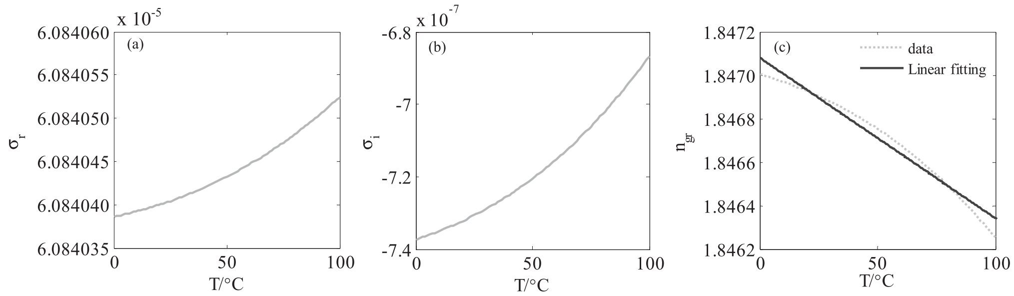

Fig. 2. (a) σ_r and (b) σ_i as a function of temperature, (c) n_{gr} as a function of temperature at $\mu_c = 0.15eV$.

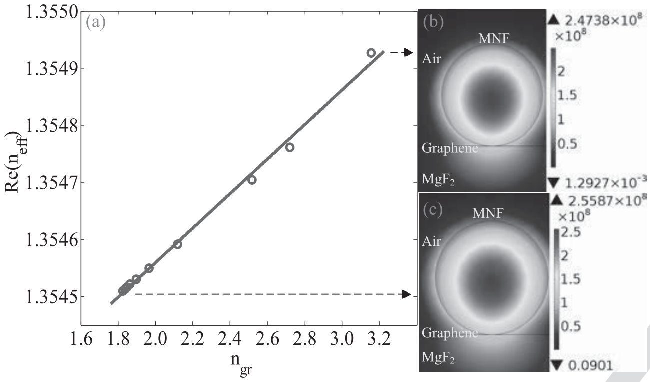

Fig. 3. (a) The real part of the effective refractive of GAMF varies with the real part of the refractive of graphene; (b) and (c) the electrical field distributions of the GAMF at Re$(n_{eff}) = 1.354926$ and Re$(n_{eff}) = 1.35451$, respectively.

index of the GAMF. The microfiber diameter is optimized around 2um both in theoretical analysis and experimental demonstration, based on the overall consideration of single mode operation [20], larger evanescent field and lower transmission loss. Here, we assume the fiber diameter is 2um, the thickness of graphene film is 1nm, the refractive indices of the MNF, MgF_2 and air are 1.44, 1.370032 and 1.0 at 20°C, respectively. Along with the reduction of n_{gr}, the real part of n_{eff} decreases linearly with the linearity of 99.6%, as depicted in Fig. 3(a). In addition, Fig. 3(b) and (c) present the optical field distribution of the GAMF at different n_{eff}. It can be seen that the central electric energy of the GAMF are respectively $2.4738 \times 10^8 V/m$ at Re$(n_{eff}) = 1.354926$ and $2.5587 \times 10^8 V/m$ at Re$(n_{eff}) = 1.35451$, which means that the transmissivity of the GAMF is linearly enhanced with the increase of the temperature. Based on the above analyses, the surrounding temperature can be simply demodulated from the variation of the transmitted optical power through the GAMF.

III. Experimental Result and Discussion

The system configuration of the GAMF based temperature sensor is illustrated in Fig. 4. The broadband optical source with optical power fluctuation less than 0.01dBm in one hour is employed to launch the light into the GAMF from port A, and the optical power meter with detection precision of 0.2dB is connected with port B of the GAMF. To precisely control the temperature variation, the GAMF sensing head is placed on the Thermoelectric Cooler (TEC). By controlling the direction and value of the operation current, the temperature can be adjusted to rise or fall between 30°C and 80°C with the step of 5°C and the resolution of 0.0625°C accurately. Then the refractive index of graphene will be changed, resulting in the variation of the transmissivity detected by the optical power meter.

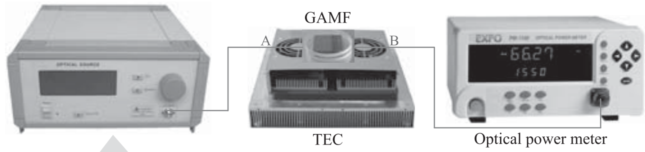

Fig. 4. Schematic diagram of the GAMF based temperature sensor system.

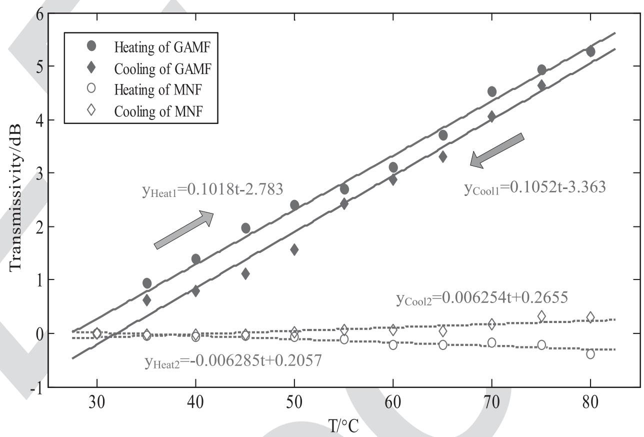

Fig. 5. Transmissivity of the fiber changes along with the temperature variation in heating procedure (amaranth) and cooling procedure (green) from 30°C to 80°C. The solid line: GAMF; the dotted line: bare MNF.

The experimental results about the sensing performance are illustrated in Fig. 5. The amaranth solid dots and line demonstrate that the transmissivity of the GAMF and the temperature possesses a direct proportional linear correlation with the sensitivity of 0.1018dB/°C. The correlation coefficient of the linear fitting curve is as high as 99.06%. According to the definition of the temperature sensitivity, i.e. $S = \Delta P/\Delta T$, the measurement resolution of temperature can be calculated as $R_T = \frac{R_P}{S}$, where S is the sensitivity of the temperature sensor, ΔP is the relative variation of the optical power, ΔT is the relative variation of the temperature, R_T is the resolution of the temperature sensor and R_P is the resolution of the optical power meter. Since the resolution of the commercial optical power meter can reach to 0.001dB, the corresponding temperature resolution is 0.0098°C.

In order to evaluate the reversibility of the sensor, the temperature detection in cooling process is also investigated. As depicted by the green solid dots and line in Fig. 5, the linear fitting of the experimental data gives a sensitivity of 0.1052dB/°C with the linearity of 98.65%. Compared with the heating process, the coincidence between the two curves confirms that the GAMF temperature sensor has good reversibility and repeatability. The deviation between the heating and cooling process data may come from the instability of the optical source, the temperature difference between graphene and TEC, and the limited measurement accuracy of the optical power meter. Although the environmental humidity will also affect the performance of graphene, the sensitivity of the GAMF sensor will be less than 0.055dB/% RH [9]. In the experiment, the room humidity keeps around 60% with the fluctuation of only 1%, resulting in the optical power variation less than 0.05dB. Therefore, the temperature measurement error induced by humidity variation is no more than 0.49°C. Furthermore, in practical applications, the sensing head can be carefully packaged to avoid the influence of the humidity, and consequently enhance the reliability and accuracy of the temperature sensor.

Furthermore, to demonstrate the sensitivity enhancement of the GAMF, we also measure the temperature response of the bare MNF in the same way as a comparison. The experimental results are presented by circles and dotted lines in Fig. 5, with very low sensitivity of −0.006285dB/°C for heating process and 0.006254dB/°C for cooling process, respectively. It is clearly that the sensitivity of GAMF is enhanced about 16 times than the bare MNF. Therefore, the assistance of graphene greatly improves the sensitivity and stability of the temperature sensor. Moreover, the sensitivity can be further enhanced by fabricating more uniform microfiber with small optical loss, appropriately adjusting the contact length between the graphene and microfiber [21], and employing the directly grown on fiber method to make the graphene film more tightly with the microfiber.

IV. Conclusion

In conclusion, an all-fiber temperature sensor based on the GAMF is proposed and demonstrated. The change of the surrounding temperature has a strong influence on the refractive index of graphene, resulting in the transmission power change in the microfiber. By simply detect the variation of the transmission power, temperature sensitivity of 0.1018dB/°C in heating process and 0.1052dB/°C in cooling process with high resolution of 0.0098°C are achieved in experiment, which is 16 times higher than that of the bare MNF. With the advantages of high sensitivity, compact size and low cost, such GAMF based sensor has great potential in sensing fields.

References

[1] L. Tong *et al.*, "Subwavelength-diameter silica wires for low-loss optical wave guiding," *Nature*, vol. 426, no. 6968, pp. 816–819, 2003.

[2] X. Zeng, Y. Wu, C. Hou, J. Bai, and G. Yang, "A temperature sensor based on optical microfiber knot resonator," *Opt. Commun*, vol. 282, no. 18, pp. 3817–3819, 2009.

[3] H. Luo, Q. Sun, Z. Xu, W. Jia, and D. Liu, "Highly sensitive temperature sensor based on D-shaped microfiber with high birefringence," *Proc. SPIE*, vol. 9157, pp. 915787-1–915787-4, Jun. 2014. AQ:1

[4] S. Zhu, F. Pang, and T. Wang, "Single-mode tapered optical fiber for temperature sensor based on multimode interference," in *Proc. IEEE ACP Asia*, Nov. 2011, pp. 1–6.

[5] S. W. Harun, K. S. Lim, S. S. A. Damanhuri, and H. Ahmad, "Microfiber loop resonator based temperature sensor," *J. Eur. Opt. Soc.-Rapid Pub.*, vol. 6, p. 11026, May 2011.

[6] Q. Bao *et al.*, "Broadband graphene polarizer," *Nature Photon.*, vol. 5, no. 7, pp. 411–415, 2011.

[7] Q. Bao *et al.*, "Graphene–polymer nanofiber membrane for ultrafast photonics," *Adv. Funct. Mater.*, vol. 20, no. 5, pp. 782–791, 2010.

[8] W. Li *et al.*, "Ultrafast all-optical graphene modulator," *Nano Lett.*, vol. 14, no. 2, pp. 955–959, 2014.

[9] Y. Xiao *et al.*, "Reduced graphene oxide for fiber-optic humidity sensing," *Opt. Exp.*, vol. 22, no. 25, pp. 31555–31567, 2014.

[10] F. Yavari, Z. Chen, A. V. Thomas, W. Ren, H.-M. Cheng, and N. Koratkar, "High sensitivity gas detection using a macroscopic three-dimensional graphene foam network," *Sci. Rep.*, vol. 1, no. 1, p. 166, 2011.

[11] J. Zhang *et al.*, "All-fiber-optic temperature sensor based on reduced graphene oxide," *Laser Phys. Lett.*, vol. 11, no. 3, p. 035901, 2014.

[12] S. Tan, H. Zhou, Y. Liu, and D. Wang, "The Characteristics and recent application progress of graphene," *World Plastics*, vol. 31, no. 7, 2013. AQ:2

[13] G. W. Hanson, "Dyadic Green's functions and guided surface waves for a surface conductivity model of graphene," *J. Appl. Phys.*, vol. 103, no. 6, p. 064302, 2008.

[14] P.-Y. Chen and A. Alù, "Atomically thin surface cloak using graphene monolayers," *ACS Nano*, vol. 5, no. 7, pp. 5855–5863, 2011.

[15] R. Yu, R. Alaee, F. Lederer, and C. Rockstuhl, "Manipulating the interaction between localized and delocalized surface plasmon-polaritons in graphene," *Phys. Rev. B*, vol. 90, no. 8, p. 085409, Aug. 2014.

[16] K. F. Mak, M. Y. Sfeir, Y. Wu, C. H. Lui, J. A. Misewich, and T. F. Heinz, "Measurement of the optical conductivity of graphene," *Phys. Rev. Lett.*, vol. 101, no. 19, p. 196405, 2008.

[17] E. Simsek, "A closed-form approximate expression for the optical conductivity of graphene," *Opt. Lett.*, vol. 38, no. 9, pp. 1437–1439, 2013.

[18] Y. Wu *et al.*, "Graphene-coated microfiber Bragg grating for high-sensitivity gas sensing," *Opt. Lett.*, vol. 39, no. 5, pp. 1235–1237, 2014.

[19] A. Feldman, D. Horowitz, R. M. Waxler, and M. J. Dodge, "Optical materials characterization," Nat. Bureau Standards Pub., Tech. Rep. 993, 1978. AQ:3

[20] A. J. Fielding, K. Edinger, and C. C. Davis, "Experimental observation of mode evolution in single-mode tapered optical fibers," *J. Lightw. Technol.*, vol. 17, no. 9, pp. 1649–1656, Sep. 1999.

[21] B. Yao *et al.*, "All-optical Mach–Zehnder interferometric NH_3 gas sensor based on graphene/microfiber hybrid waveguide," *Sens. Actuators B, Chem.*, vol. 194, pp. 142–148, Apr. 2014.